9.18 Multiplane Stereo PIV

Contributed by:
C.J. Kähler

9.18.1 Introduction

Particle Image Velocimetry (PIV) has become a widely applied technique whenever the spatial distribution of the velocity together with its derivatives helps to understand the physics of the flow. However, quite often the distribution of the velocity within one single plane, captured at one instant in time, does not yield the information required to answer fluid-mechanical questions. To overcome these limitations a stereoscopic PIV based technique has been developed, which is well suited to determine many fluid-mechanical quantities with high accuracy and spatial resolution at any flow velocity [200, 390, 392, 393]. This technique is reliable, robust and easy to handle. Furthermore it is based on standard PIV equipment and evaluation procedures so that available PIV systems can be easily extended.

The multiplane stereo PIV system, developed for applications in air flows in particular, consists of a four-pulse laser system delivering orthogonally polarized light, two pairs of high resolution progressive scan CCD cameras in an angular imaging configuration with Scheimpflug correction, two high reflectivity mirrors and a pair of polarizing beam-splitter cubes according to figure 9.85.

After the illumination of the tracer particles with orthogonally linearly polarized light, the polarizing beam-splitter cube (7) separates the incident

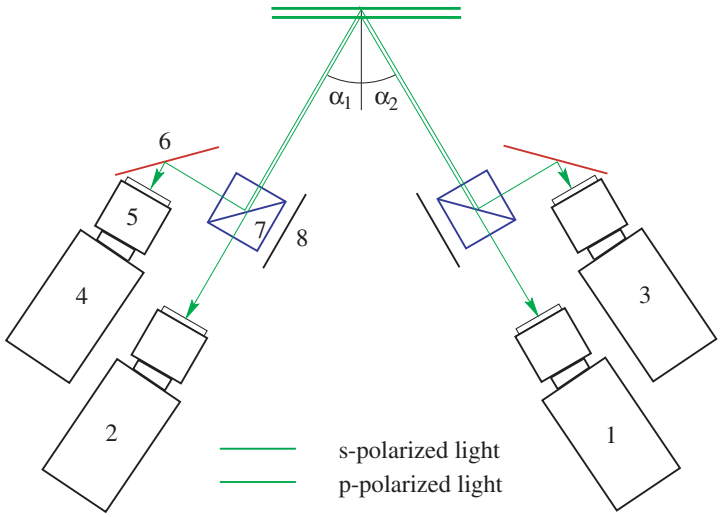

Fig. 9.85. Schematic setup of the recording system. 1-4 digital cameras, 5 lens, 6 mirror, 7 polarizing beam-splitter cube with dielectric coating between the two right-angle prisms, 8 absorbing material, α opening angle.

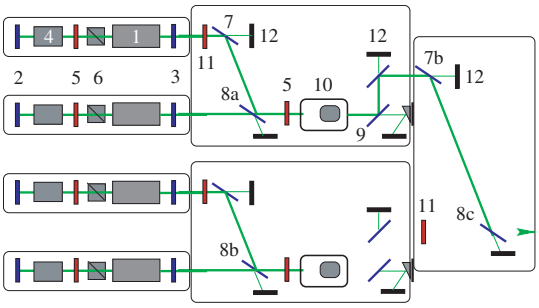

Fig. 9.86. Four-pulse four frequency Doppler laser system. 1 Pump cavity, 2 Full reflective mirror, 3 Partially transmitting mirror, 4 Pockels cell, 5 $\lambda/4$ retardation plate, 6 Glan-Laser polarizer, 7 Mirror, 8 Dielectric polarizer, 9 Dichroic mirror, 10 Frequency doubler crystal with phase angle adjustment, 11 $\lambda/2$ retardation plate, 12 Beam dump.

wave-front scattered from the particles into two parts according to the state of polarization. The separation based on polarization works perfectly as long as the radius of the spherical particles is comparable to the wavelength of the laser light (see also section 2.1 and [72, 73] for the generation of appropriate particles) and the observation direction is properly aligned relative to the direction of the polarization vector. In the case that these requirements cannot be fulfilled a frequency based multiplane stereo PIV approach can be applied but in this case the laser system has to be modified to generate the required frequency shift [395].

For the illumination of the tracer particles the beams of four independent laser-oscillators need to be combined in such a way that the linearly polarized light sheets can be positioned independently with respect to each other. This can be easily and precisely done by means of the four pulse system shown in figure 9.86.

The appropriate method of adjusting the displacement between the orthogonally polarized light-sheets depends on the desired distance [389, 390]. Small separations between the orthogonally polarized light-sheet pairs (up to a few millimeters) can be generated by a simple rotation of mirror 8c in the re-combination optics around the axis perpendicular to the laser-beam plane [393]. For a wider range of light-sheet spacings (up to a few cm) and independent positioning of both beam-pairs, it is useful to remove mirror 7b along with the beam dump (12) such that two spatially separated laser beams with orthogonally polarized radiation emerge. Using two separate light-sheet-optics (one for each polarization) each with a 45° mirror behind the last lens, all positions are possible by moving the mirrors [389]. Once calibrated, the actual position of each pair of light-sheets is determined with a micrometer scale.

The multiple plane stereo system is well suited to determine different fluid-mechanical quantities without perspective error simply by changing the time sequence or light sheet position. For constant pulse separation ($\Delta t = t_2 - t_1 = t_3 - t_2 = t_4 - t_3$) and overlapping light sheets (see figure 9.87), a time

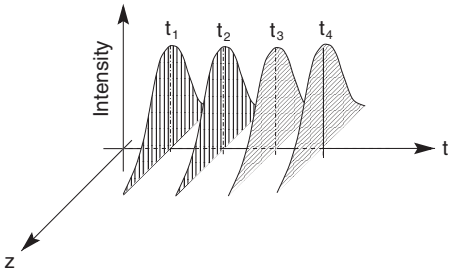

Fig. 9.87. Timing diagram for the temporally separated determination of all three velocity components. Different shading of the light-sheet profile indicates different states of polarization.

sequence of three velocity fields can be measured at any flow velocity by cross-correlating the first acquired gray-level distribution with the second, the second with the third and the third with the gray-level distribution from the last illumination. In this mode it is also possible to increase the accuracy of the velocity measurement by using the Multiframe PIV evaluation approach outlined in section 9.7 and [323]. By increasing the time delay between the second and third illumination ($\Delta t = t_2 - t_1 = t_4 - t_3 < t_3 - t_2$) the first order estimation of the acceleration field in its Lagrangian and Eulerian form can be calculated to study the dynamic behavior and the interaction processes of moving flow structures [388]. For large time delays between a pair of images being acquired ($\Delta t = t_2 - t_1 = t_4 - t_3 \ll t_3 - t_2$), time correlations can be measured for instance [389].

When the light sheet pairs with equal polarization are spatially separated, as indicated in figure 9.88, further important information about the flow field can be achieved. For small separations or partially overlapping light-sheets, the spatial distribution of all three vorticity vector components can be measured when the orthogonal polarized light-pulses are fired simultaneously ($t_1 = t_3$ and $t_2 = t_4$). In addition, all components of the velocity gradient tensor can be estimated along with the invariants of this tensor [390, 396]. This allows vortex identification to be made more reliably in combination with topological flow analysis. By increasing the distance between the light sheet pairs, the spatial correlation tensor at different locations within the flow field

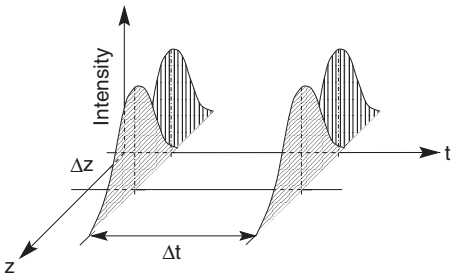

Fig. 9.88. Timing diagram for the simultaneous determination of all three velocity components in spatially separated planes.

can be measured [394]. Furthermore the orientation of a vortex crossing the planes can be determined precisely which is of major importance for aircraft wake-vortex investigations for example. Time-correlations can also be deduced from the data by varying the time between the horizontal and vertical pairs of illuminations [389].

9.18.2 Application

To demonstrate the capabilities of the technique a flat-plate boundary layer flow was examined in stream-wise span-wise planes located at $y^+ = 10$, $y^+ = 20$ and $y^+ = 30$. The experimental investigation was performed 18 m behind the leading edge of the flat plate placed in the temperature-stabilized closed circuit wind tunnel at the Laboratoire de Mécanique de Lille (LML), see [386] for details. The flow and recording parameter are listed in table 9.22.

Table 9.22. Relevant parameters for the characterization of the experiment performed 18 m behind the leading edge of the flat plate in the xz-plane (stream-wise span-wise) of the turbulent boundary layer flow.

Re_θ	7800 [1]
Re_δ	74000 [1]
Re_x	3.6×10^6 [1]
U_∞	3 [m/s]
u_τ	0.121 [m/s]
δ	0.37 [m]
δ^+	3000 [1]
$t^+ = tu_\tau^2/\nu$	[1]
field of view	67×35 [mm^2]
field of view	0.18×0.09 [δ^2]
field of view	544×284 [$\Delta x^+ \Delta z^+$]
spatial resolution	$1.42 \times 0.6 \times 1.42$ [mm]
spatial resolution	$11.5 \times 5.0 \times 11.5$ [$\Delta x^+ \Delta y^+ \Delta z^+$]
pulse separation Δt	200 [μs]
dynamic range at $y^+ = 10$	1.00 to 9.330 [pixel]
dynamic range at $y^+ = 20$	1.37 to 11.74 [pixel]
dynamic range at $y^+ = 30$	2.61 to 11.84 [pixel]
vectors per sample	7936
number of samples	4410

For phenomena associated with the production of turbulence, the cross correlation between the fluctuating stream-wise u and the wall-normal v velocity components, measured simultaneously at different y^+-locations, is very important, as R_{vu} reflects the size and shape of the coherent flow structures being responsible for the transport of relatively low-momentum fluid outwards

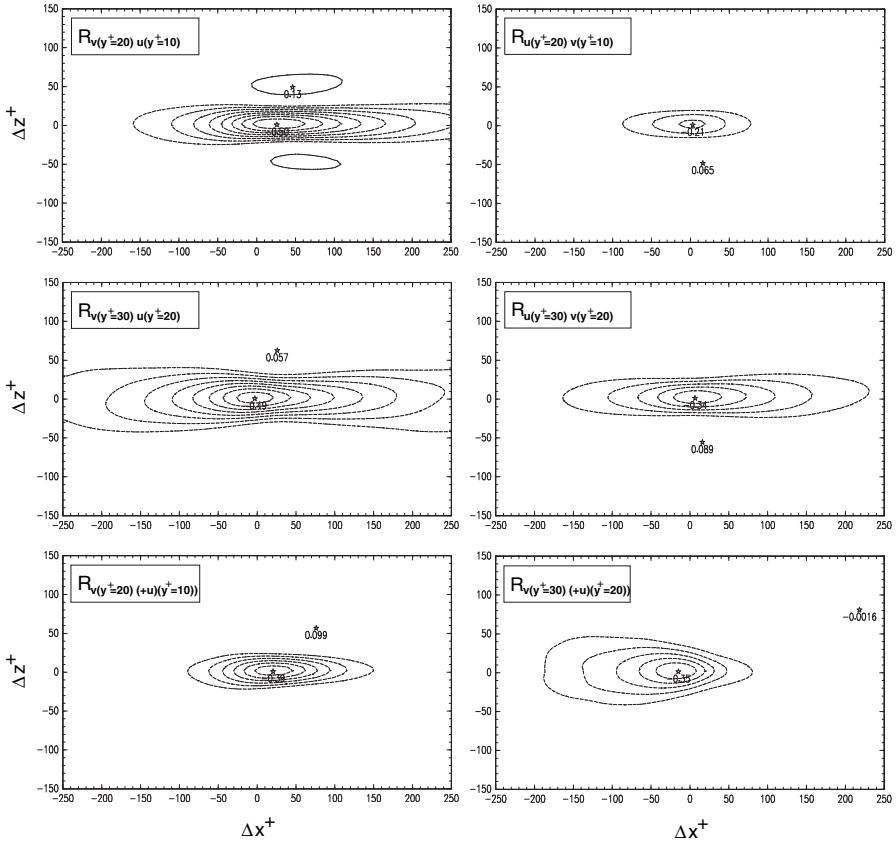

Fig. 9.89. Two-dimensional spatial cross-correlation function of fluctuating streamwise (u) with wall-normal (v) velocity components measured at $Re_\theta = 7800$. *Top:* $R_{v(y^+=20)u(y^+=10)}$ (*left*) and $R_{u(y^+=20)v(y^+=10)}$ (*right*). *Centre:* $R_{v(y^+=30)u(y^+=20)}$ (*left*) and $R_{u(y^+=30)v(y^+=20)}$ (*right*). *Bottom:* $R_{v(y^+=20)u(y^+=10)}$ with $u > 0$ (*left*) and $R_{v(y^+=30)u(y^+=20)}$ with $u > 0$ (*right*).

into higher speed regions and for the movement of high-momentum fluid toward the wall and into lower speed regions.

Figure 9.89 displays the statistical relation between the fluctuating velocity components. The top row shows the cross-correlation $R_{v(y^+=20)u(y^+=10)}$ (left) and $R_{u(y^+=20)v(y^+=10)}$ (right). It can be stated from the negative sign of the correlation, indicated by the dashed lines, that the ejection and sweeps must be the predominant processes and the different size, shape and intensity of the functions ($R_{v(y^+=20)u(y^+=10)} > R_{u(y^+=20)v(y^+=10)}$) imply the dominance of ejection at these wall locations. In addition, it can be estimated from the location of the maximum in the upper left graph that the low momentum region appears as a shear layer in the y-direction while the strong positive side

peaks in the same figure indicate that the outflow of low-momentum fluid is associated with a secondary motion. The center row of figure 9.89 reveals the same functions but measured at $y^+ = 20$ and $y^+ = 30$ e.g. $R_{v(y^+=30)u(y^+=20)}$ (left) and $R_{u(y^+=30)v(y^+=20)}$ (right). The bottom row of figure 9.89 yields the conditional cross-correlation $R_{v(y^+=20)u(y^+=10)}$ with $u > 0$ (left) and $R_{v(y^+=30)u(y^+=20)}$ with $u > 0$ (right). Especially the amplitude of R_{vu} in the lower right plot should be noted. To estimate the convection velocity of the various coherent flow structures, and further dynamical aspects which are not accessible by using standard, stereoscopic or holographic PIV techniques, space-time correlations were measured in addition. See [389, 390, 391] for details.

9.18.3 Conclusion

The Multiplane Stereo PIV system is very reliable, robust and well suited for all kinds of applications, purely scientific as well as for industrially motivated investigations in large wind tunnels where acquisition time, optical access and observation distances are constrained. Furthermore, it is based on the conventional PIV equipment and the familiar evaluation procedure so that available PIV systems can easily be expanded. The advantage of this measurement system with respect to other imaging techniques lies in its ability to determine a variety of fundamentally important fluid-mechanical quantities with high accuracy (no perspective error), simply by changing the time sequence or light sheet position. Due to the advantage of this technique relative to conventional PIV systems, it is increasingly applied by other leading research groups all over the world [385, 387, 396].